Impact of dopant compensation on the deactivation of boron-oxygen recombination centers in crystalline silicon

Bianca Lim,[1,a)] An Liu,[2] Daniel Macdonald,[2] Karsten Bothe,[1] and Jan Schmidt[1]
[1]*Institut für Solarenergieforschung Hameln (ISFH), Am Ohrberg 1, D-31860 Emmerthal, Germany*
[2]*School of Engineering, College of Engineering and Computer Science, The Australian National University, Canberra ACT 0200, Australia*

(Received 16 September 2009; accepted 19 November 2009; published online 10 December 2009)

The boron-oxygen recombination center responsible for the light-induced degradation of Czochralski silicon solar cells can be permanently deactivated by illumination at elevated temperature. In this study, we examine the impact of dopant compensation on the deactivation process. The experimental results show that the deactivation rate depends inversely on the total boron concentration instead of the net doping concentration, suggesting that boron is directly involved in the deactivation process. A linear dependence of the activation energy on the total boron concentration further supports this conclusion. © *2009 American Institute of Physics*.
[doi:10.1063/1.3272918]

Recombination-active boron-oxygen complexes form in boron-doped Czochralski-grown silicon (Cz-Si) under illumination at room temperature. These complexes typically limit the carrier lifetime in oxygen-rich silicon.[1] As a consequence, solar cells fabricated on B-doped Cz-Si suffer from a loss in energy conversion efficiency of up to 10% relative.[2,3] A permanent deactivation of the defect can be achieved through illumination at elevated temperature.[4–6] The deactivation process was found to be thermally activated and activation energies between 0.61 (Refs. 4 and 5) and 0.71 eV (Ref. 6) have been reported.

In this work, we present carrier lifetime measurements aimed at investigating the impact of dopant compensation on the deactivation process and find that the deactivation rate is inversely proportional to the total boron concentration. In addition, a linear dependence of the activation energy on the total boron concentration is revealed. Both results provide strong evidence that boron plays a role in the deactivation process.

We examine Cz-Si wafers from five different ingots, three are exclusively doped with boron (noncompensated controls) and two ingots are doped with boron and phosphorus. The resistivities ρ of the noncompensated reference wafers are 5.8, 1.26, and 0.45 Ω cm, as measured by the four-point-probe method after thermal donor annihilation. The resistivities of the compensated samples are 1.20 and 0.52 Ω cm, respectively.

Using the model of Klaassen[7,8] (assuming a temperature of 25 °C), we subsequently determine the hole mobility μ_{hK} and the equilibrium hole concentration $p_{0\rho}$ in the noncompensated samples via a self-consistent calculation. The obtained values are summarized in Table. I. The hole concentrations in the wafers are additionally determined by electrochemical capacitance voltage (ECV) measurements[9] and we find very good agreement between p_{0ECV} and $p_{0\rho}$ (see Table I).

To determine the boron (N_A) and the phosphorus concentrations (N_D) in the compensated samples, we use a method introduced by Macdonald *et al.*,[10] which is based on the measurement of the association time constant τ_{assoc} of iron-boron (FeB) pairs. Since no interstitial iron can be detected in the as-grown samples, we transfer iron from Fe-contaminated multicrystalline silicon wafers during a high-temperature anneal at 1000 °C to the monocrystalline Cz-Si wafers.[11] The same measurements are also performed on the noncompensated wafers, where the hole concentration p_0 equals the acceptor concentration N_A, i.e., the density of substitutional boron. As can be seen from Table I, for the noncompensated samples the values of N_A from the τ_{assoc}

TABLE I. Resistivities ρ as measured by the four-point-probe method, hole mobilities μ_{hK} in the noncompensated wafers from Klaassen's model, equilibrium hole concentration $p_{0\rho}$ determined from ρ and μ_{hK}, equilibrium hole concentration p_{0ECV} determined via ECV measurements, and the acceptor concentration N_A measured via the iron-acceptor repairing time constants τ_{assoc}.

Wafer	ρ from four-point-probe [Ω cm]	Hole mobility μ_{hK} (Klaassen) [$cm^2/V\,s$]	$p_{0\rho}$ from ρ and μ_{hK} [cm^{-3}]	p_{0ECV} from ECV [cm^{-3}]	N_A from τ_{assoc} [cm^{-3}]
74 (noncompensated)	5.8	462	2.33×10^{15}	⋯	3.37×10^{15}
72 (noncompensated)	1.26	431	1.15×10^{16}	1.14×10^{16}	1.85×10^{16}
73 (noncompensated)	0.45	384	3.61×10^{16}	3.8×10^{16}	3.35×10^{16}
45 (compensated)	1.20	⋯	⋯	1.5×10^{16}	3.0×10^{16}
44 (compensated)	0.52	⋯	⋯	4.1×10^{16}	9.2×10^{16}

a)Electronic mail: lim@isfh.de.

TABLE II. Resistivities ρ of the compensated samples as measured by the four-point-probe method, equilibrium hole concentration p_{0ECV} determined via ECV measurements, acceptor concentration N_A measured via the iron-acceptor repairing time constants τ_{assoc}, phosphorus concentration $N_D=N_A-p_{0ECV}$, hole mobilities μ_{hK} from Klaassen's model using N_A and N_D, measured hole mobilities $\mu_h \equiv (\rho\ e\ p_{0ECV})^{-1}$, equilibrium hole concentration $p_{0\rho} \equiv (\rho\ e\ \mu_{hK})^{-1}$, and the compensation level $C=(N_A+N_D)/(N_A-N_D)$.

Wafer	ρ from four-point-probe [Ω cm]	p_{0ECV} from ECV [cm^{-3}]	N_A from τ_{assoc} [cm^{-3}]	$N_D=N_A-p_{0ECV}$ [cm^{-3}]	Hole mobility μ_{hK} (Klaassen) [$cm^2/V\ s$]	Measured μ_h [$cm^2/V\ s$]	$p_{0\rho}$ from ρ and μ_{hK} [cm^{-3}]	$C=\frac{N_A+N_D}{N_A-N_D}$
45 (compensated)	1.20	1.5×10^{16}	3.0×10^{16}	1.5×10^{16}	380	347	1.37×10^{16}	3
44 (compensated)	0.52	4.1×10^{16}	9.2×10^{16}	5.1×10^{16}	306	293	3.92×10^{16}	3.5

measurements are in good agreement with the hole concentrations p_{0ECV} and $p_{0\rho}$.

Knowing the boron concentrations N_A, the phosphorus concentrations N_D in the compensated samples then follow from $N_D=N_A-p_{0ECV}$ to be 1.5×10^{16} cm^{-3} for the 1.20 Ω cm wafer and 5.1×10^{16} cm^{-3} for the 0.52 Ω cm wafer, as summarized in Table II. The compensation level $C=(N_A+N_D)/(N_A-N_D)$ in the 0.52 Ω cm wafer is thus higher than in the 1.20 Ω cm sample (3.5 and 3, respectively). Looking at the measured hole mobility $\mu_h \equiv (\rho\ e\ p_{0ECV})^{-1}$, where e is the elementary charge, we find a reduction in majority carrier mobility with an increase in compensation level ($\mu_h=347$ cm^2/Vs in the 1.20 Ω cm compensated wafer and $\mu_h=293$ cm^2/Vs in the compensated 0.52 Ω cm material). This reduction is in good agreement with Klaassen's model,[7,8] which yields $\mu_{hK}=380$ cm^2/Vs in the 1.20 Ω cm compensated material and $\mu_{hK}=306$ cm^2/Vs in the 0.52 Ω cm samples. Table II also includes the hole concentrations $p_{0\rho}$ as given by $p_{0\rho} \equiv (\rho\ e\ \mu_{hK})^{-1}$, which are in very good agreement with the hole concentrations determined via ECV measurements.

For lifetime measurements the samples were cleaned and underwent a phosphorus-diffusion step to remove metal impurities. Prior to passivation with plasma-enhanced chemical vapor deposited silicon nitride,[12] the n^+ regions on both surfaces were removed by wet chemical etching.

Illumination at elevated temperature was performed on a hotplate with a halogen lamp. The light intensity was adjusted with a calibrated solar cell while the temperature was controlled by a proportional-integral-derivative-controller. All stated temperatures refer to the set temperature, leading to an error in the actual temperature of up to 5 °C. Carrier lifetimes were measured at room temperature using the quasi-steady-state photoconductance technique.[13]

Samples from the five different ingots were cured at 185 °C and at a light intensity of 100 mW/cm^2. Figure 1 shows the normalized defect concentration N_t^* of the 1.26 Ω cm noncompensated control and the 1.20 Ω cm compensated sample plotted against the duration of illumination t. N_t^* is defined as the difference of the inverse lifetime $\tau^{-1}(t)$ measured at time t and the inverse initial lifetime measured before degradation τ_0^{-1}, i.e., $N_t^*=\tau^{-1}(t)-\tau_0^{-1}$. For better comparison, $N_{t.max}^*$ is furthermore normalized to one. The deactivation rate R_{de} is determined by fitting a curve of the form $N_t^*(t)=A\times\exp(-R_{de}t)+B$ to the measured data (solid lines in Fig. 1). The difference between the noncompensated wafer (filled green circles) and the compensated sample (open purple squares) in Fig. 1 is obvious; the deactivation in the compensated sample takes three times longer than in the noncompensated wafer. Comparing the 0.45 Ω cm control wafer and the 0.52 Ω cm compensated sample we find a similar decrease in the deactivation rate by a factor of 2.4 (not plotted).

The deactivation rates R_{de} determined at 185 °C and at a light-intensity of 100 mW/cm^2 are plotted versus the total boron concentration N_A in Fig. 2 (filled symbols). The double-logarithmic scale reveals a reciprocal dependence of the deactivation rate on the boron concentration for the noncompensated controls (filled blue triangles up). The fit yields a slope of −0.74, i.e., $R_{de}\sim N_A^{-0.74}$. Plotting the deactivation rate of the compensated samples versus the hole concentration p_0 (open red triangles down) results in a considerable deviation from the fit. However, if the deactivation rate is plotted as a function of the total boron concentration N_A (filled red triangles down), there is good agreement with the fit to the data of the noncompensated wafers. The observed dependence of the deactivation rate R_{de} on the total boron concentration N_A in compensated silicon, in contrast to a dependence on the hole concentration $p_0=N_A-N_D$, is a strong indication that boron plays a role in the deactivation process. With regard to the proposed formation of boron-phosphorus pairs in compensated silicon,[14–16] this finding also implies that the involvement of boron is irrespective of its chemical bonding state.

Further deactivation experiments were performed at 140, 165, and 200 °C. Figure 3 depicts the respective deactivation rates R_{de} of the 1.26 Ω cm control and the 1.20 Ω cm compensated wafers in an Arrhenius plot. It can be seen that the deactivation rate of the noncompensated wafer is higher

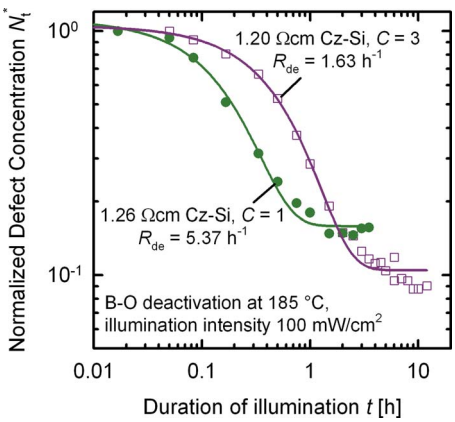

FIG. 1. (Color online) Time dependence of the normalized defect concentration N_t^* in two samples during illumination at 185 °C on a double-logarithmic scale. The filled green circles refer to a 1.26 Ω cm boron-doped noncompensated Cz-Si wafer, whereas the open purple squares correspond to a 1.20 Ω cm compensated (B- and P-doped) Cz-Si sample. The data is fitted by an exponential decay function which yields the deactivation rate R_{de}. A clear decrease of R_{de} for the compensated wafer can be seen.

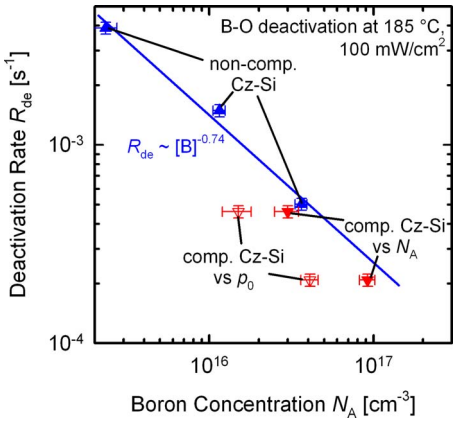

FIG. 2. (Color online) Deactivation rates R_{de} determined at 185 °C of noncompensated Cz-Si control wafers (filled blue triangles up) are plotted on a double-logarithmic scale vs the total boron concentration N_A. The fit with a power law (blue line) yields an exponent of −0.74. The deactivation rates of the compensated Cz-Si wafers are plotted against the net-doping concentration p_0 (open red triangles down) and the total boron concentration N_A (filled red triangles down). The agreement with the fit is much better for the latter.

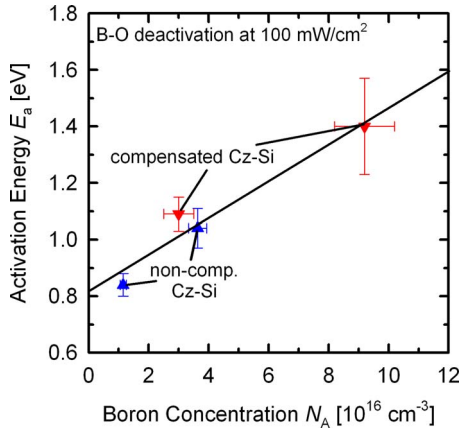

FIG. 4. (Color online) Activation energies E_a of the noncompensated reference wafers (filled blue triangles) and the compensated samples (filled red triangles) plotted vs the total boron concentration N_A, showing a linear relationship between E_a and N_A.

than that of the compensated sample at all temperatures. In addition, the fits yield different slopes, which means that they result in two different activation energies E_a. So far activation energies between 0.61 (Refs. 4 and 5) and 0.71 eV (Ref. 6) have been reported for silicon with a resistivity of about 1.4 Ω cm. This is slightly less than the value of 0.84 eV for the 1.26 Ω cm noncompensated sample found in this study. The activation energy of the 1.20 Ω cm compensated sample is 1.09 eV, however, which is 30% above the corresponding E_a of the noncompensated reference sample. The 0.45 Ω cm control yields a comparable value E_a=1.04 eV, whereas the compensated 0.52 Ω cm Cz-Si material has an even higher activation energy of 1.40 eV. Plotting the activation energies E_a of all investigated samples as a function of the total boron concentration N_A, as depicted in Fig. 4, we find a linear dependence between E_a and N_A. The observed linear correlation between E_a and N_A provides additional evidence that boron is directly involved in the deactivation process.

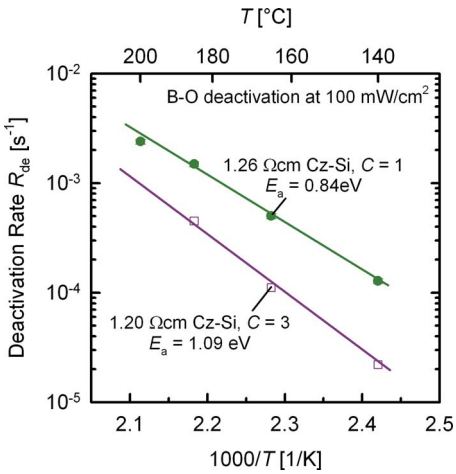

FIG. 3. (Color online) Arrhenius-plot of the deactivation rates R_{de} of a 1.26 Ω cm noncompensated Cz-Si sample (filled green circles) and a 1.20 Ω cm compensated Cz-Si wafer (open purple squares). The activation energy E_a derived for the compensated wafer is 30% above that of the control sample.

In this study, we have shown that the permanent deactivation of the boron-oxygen-related recombination center also works in compensated silicon. The comparison with noncompensated control wafers revealed that the deactivation rate R_{de} in compensated silicon depends on the total boron concentration N_A rather than on the hole concentration p_0. An examination of the activation energy E_a showed a linear correlation of E_a with N_A instead of a correlation with p_0. Both experimental findings provide strong evidence that boron plays a role in the deactivation process and that its involvement is irrespective of its chemical bonding state.

Funding was provided by the State of Lower Saxony and the DAAD/Go8 Australia Germany Joint Research Cooperation Scheme.

[1] J. Schmidt and K. Bothe, Phys. Rev. B **69**, 024107 (2004).
[2] H. Fischer and W. Pschunder, *Proceedings of the Tenth IEEE Photovoltaic Specialists Conference*, Palo Alto, CA (IEEE, New York, 1973), p. 404.
[3] J. Knobloch, S. W. Glunz, V. Henninger, W. Warta, W. Wettling, F. Schomann, W. Schmidt, A. Endrös, and K. A. Münzer, *Proceedings of the 13th European Photovoltaic Solar Energy Conference*, Nice, France (Stephens, Bedford, 1995), p. 9.
[4] A. Herguth, G. Schubert, M. Kaes, and G. Hahn, *Proceedings of the 21st European Photovoltaiv Solar Energy Conference*, Dresden, Germany (WIP, Munich, 2006), p.530.
[5] A. Herguth, G. Schubert, M. Kaes, and G. Hahn, Prog. Photovoltaics **16**, 135 (2008).
[6] B. Lim, K. Bothe, and J. Schmidt, Phys. Status Solidi (RRL) **2**, 93 (2008).
[7] D. B. M. Klaassen, Solid-State Electron. **35**, 953 (1992).
[8] D. B. M. Klaassen, Solid-State Electron. **35**, 961 (1992).
[9] R. Bock, P. P. Altermatt, and J. Schmidt, *Proceedings of the 23rd European Photovoltaics Solar Energy Conference*, Valencia, Spain (WIP, Munich, 2008), p. 1510.
[10] D. Macdonald, A. Cuevas, and L. J. Geerligs, Appl. Phys. Lett. **92**, 202119 (2008).
[11] D. Macdonald, M. Kerr, and A. Cuevas, Appl. Phys. Lett. **75**, 1571 (1999).
[12] T. Lauinger, J. Schmidt, A. G. Aberle, and R. Hezel, Appl. Phys. Lett. **68**, 1232 (1996).
[13] R. Sinton and A. Cuevas, Appl. Phys. Lett. **69**, 2510 (1996).
[14] S. Pizzini and C. Calligarich, J. Electrochem. Soc. **131**, 2128 (1984).
[15] R. Kopecek, J. Arumughan, K. Peter, E. A. Good, J. Libal, M. Acciarri, and S. Binetti, *Proceedings of the 23rd European Photovoltaics Solar Energy Conference*, Valencia, Spain (WIP, Munich, 2008), p. 1855.
[16] D. Macdonald, F. Rougieux, A. Cuevas, B. Lim, J. Schmidt, M. Di Sabatino, and L. J. Geerligs, J. Appl. Phys. **105**, 093704 (2009).